

Impact of aromatics and monoterpenes on simulated tropospheric ozone and total OH reactivity



William C. Porter*, Sarah A. Safieddine, Colette L. Heald

Department of Civil and Environmental Engineering, Massachusetts Institute of Technology, 77 Massachusetts Avenue, Cambridge, MA 02139-4307, USA

HIGHLIGHTS

- Impacts of aromatics and monoterpenes estimated using chemical transport model.
- Large increases in surface O_3 predicted at extremely VOC-sensitive locations.
- Computational cost could be mitigated through simplified chemistry schemes.

ARTICLE INFO

Article history:

Received 12 May 2017

Received in revised form

18 August 2017

Accepted 20 August 2017

Available online 31 August 2017

Keywords:

Tropospheric ozone

VOCs

Atmospheric chemistry

Air quality modeling

ABSTRACT

The accurate representation of volatile organic compounds (VOCs) in models is an important step towards the goal of understanding and predicting many changes in atmospheric constituents relevant to climate change and human health. While isoprene is the most abundant non-methane VOC, many other compounds play a large role in governing pollutant formation and the overall oxidative capacity of the atmosphere. We quantify the impacts of aromatics and monoterpenes, two classes of VOC not included in the standard gas-phase chemistry of the chemical transport model GEOS-Chem, on atmospheric composition. We find that including these compounds increases mean total summer OH reactivity by an average of 11% over the United States, Europe, and Asia. This increased reactivity results in higher simulated levels of O_3 , raising maximum daily 8-h average O_3 in the summer by up to 14 ppb at some NO_x -saturated locations.

© 2017 Elsevier Ltd. All rights reserved.

1. Introduction

Volatile organic compounds (VOCs) play a critical role within the Earth's troposphere, affecting the global climate, controlling the formation of common pollutants, and influencing the lifetimes of other key atmospheric compounds. VOCs are emitted from both natural and anthropogenic sources, including combustion and industrial production processes (Piccot et al., 1992), as well as natural emissions from trees and other plant life (Guenther et al., 2012). The accurate representation of these compounds within atmospheric models is a key goal of the atmospheric chemistry community, largely because they are direct precursors of ozone (O_3) and fine particulate matter ($PM_{2.5}$), known pollutants which can also influence the global climate (Jenkin and Clemmshaw, 2000). VOCs also have major impacts on other key atmospheric species,

including the hydroxyl radical (OH), one of the key contributors to the oxidation capacity of the atmosphere.

Tropospheric O_3 is an EPA criteria pollutant responsible for an estimated 200,000 premature mortalities worldwide each year (Lim et al., 2012). Ozone concentrations are typically highest on hot, stagnant days in the presence of abundant nitrogen oxides (NO_x) and VOCs. While there has been some success in reducing the magnitude of extreme summertime O_3 events across the United States and Europe, especially in urban areas (Guerreiro et al., 2014; Simon et al., 2015), difficulties in predicting and reducing global tropospheric O_3 levels remain (Cooper et al., 2014). Among the causes of these difficulties are uncertainties surrounding the emissions, chemistry, and removal of VOCs and other O_3 precursors, especially due to the non-linearity of the relationship between precursor concentrations and O_3 production. Understanding spatial and temporal variability in atmospheric oxidative capacity, O_3 formation rates, and other consequences of VOCs will require that gap to be closed, both in ambient observations of the atmosphere and within the models used to represent it. Many studies have reported

* Corresponding author.

E-mail address: wporter@mit.edu (W.C. Porter).

a gap between summed observed OH reactivity and observations based on OH lifetimes, a discrepancy which could be explained by the presence of unidentifiable VOCs and/or their oxidation products (Yang et al., 2016). Meanwhile, although the current generation of chemical transport models typically includes a variety of species representing the most common and influential VOCs, this is a small fraction of the 3000–4000 currently identifiable species, which is, in turn, only a small fraction of the total compounds (estimated to be on the order of 10^4 – 10^5) present in the atmosphere (Goldstein and Galbally, 2007).

GEOS-Chem, a model often used for the study of pollutants and tropospheric composition, simulates the emission and oxidation of many of the most important atmospheric non-methane VOC (NMVOC) classes, including natural compounds such as isoprene, monoterpenes, and sesquiterpenes, as well as anthropogenically emitted compounds such as the aromatics benzene, toluene, and xylene. However, while all of these species contribute to modeled PM_{2.5} through the formation of secondary organic aerosol (SOA, Pye et al., 2010), only isoprene, the most abundant of the VOCs, is included in the standard gas-phase chemical mechanism. This represents a gap in modeled OH reactivity, with potential consequences on the accuracy of predicted O₃ formation, OH lifetimes, and other related species.

2. Methodology

To explore the impact of aromatics and monoterpenes on tropospheric chemistry, we use the chemical transport model GEOS-Chem (www.geos-chem.org) v9-02, modified to include additional VOC species within the gas-phase chemical mechanism. We performed two years of global simulations (2010 and 2011) using a 2° x 2.5° horizontal resolution and 47 vertical levels. We also use these global simulations to produce boundary conditions for higher resolution (0.5° x 0.6°) nested regional simulations over North America, Europe, and Asia. With high O₃ events primarily a summertime phenomenon, we focus on the months of June, July, and August in our figures and analyses.

To better represent the chemical impacts of monoterpenes and aromatics, the GEOS-Chem gas-phase chemical mechanism was modified using mechanisms from Knote et al., 2014 for aromatics and Fisher et al., 2016 for monoterpenes as part of a larger effort to track total reactive carbon with GEOS-Chem (Safieddine et al., 2017). To this end, we bring several aromatic and monoterpene species (previously included only as contributors to SOA formation) online with respect to OH reactivity and O₃ formation, tracking several generations of oxidation products. These additions build upon the existing isoprene oxidation scheme (Paulot et al., 2009b, 2009a), providing a fuller representation of VOC chemistry and ozone formation. All added species are shown on the left-hand side of Table 1, and include the aromatics benzene, toluene, and xylene, along with two lumped monoterpene tracers representing α -pinene, β -pinene, sabinene, Δ -3-carene, limonene, myrcene, and ocimene. These two sets of modifications were made separately in individual simulations (AROM and TERP), as well as combined together in merged simulations (FULL) including all 42 additional compounds (32 associated with aromatics and 10 with monoterpenes). In addition to these three cases, we evaluate a simplified mechanism (SIMPLE) that delivers much of the total increased OH reactivity of the FULL set, with only 14 additional species, and therefore less computational overhead. These two additional mechanisms represent increases of 45% and 15%, respectively, over the original 93 species in the base GEOS-Chem mechanism. The tracers added to the SIMPLE cases, along with their literature sources, are listed on the right-hand side of Table 1. We compare these modified cases to base simulations (BASE) which lack the

additional chemistry of the test cases, but are otherwise identical.

We use standard inventories for most emissions, including EDGARv3 for CO, NO_x, and SO_x, along with RETRO for VOCs other than ethane, including benzene, toluene, and xylene – the aromatics examined in this work (Olivier and Berdowski, 2001; Pulles et al., 2007). We take ethane emissions from (Xiao et al., 2008). Where available, high resolution regional alternatives are used in place of global inventories, including the EPA's NEI2005 inventory over the United States, the CAC inventory over Canada, BRAVO for emissions over Mexico (Kuhns et al., 2005), EMEP emissions over Europe (Auvray and Bey, 2005), and the Streets 2006 inventory for Asia (Zhang et al., 2009). In following with recent literature results suggesting that NEI NO_x emissions are too high by a factor of 2, we reduce anthropogenic NO_x emissions over the United States following the recommendations of Travis et al. (2016), after first scaling up the NEI2005 emissions to match NEI2011 totals for the years 2010 and 2011. Global emissions from biomass burning are taken from the GFED3 inventory, while biogenic emissions (including those of the additional monoterpene species) are calculated online using MEGAN v2.02 (Mu et al., 2011; Guenther et al., 2006).

For comparison to observations in the United States, we use hourly station O₃ data taken from the EPA's AQS network (US Environmental Protection Agency) to calculate daily maximum 8-h averages.

3. Results

3.1. Increases in summer surface OH reactivity

The inclusion of aromatics and monoterpenes increases the simulated total summertime surface OH reactivity, with rural increases largely resulting from new monoterpene reactivity, and urban centers showing aromatic-driven changes. In the United States (Fig. 1), regional reactivity peaks in the southeast, coincident with extremely high rates of biogenic emissions. Highest relative changes in OH reactivity occur over regions where both anthropogenic and natural emissions are present. For example, OH reactivity increases by 20–30% over much of the southeast, which sees overall reactivity increases of over 2 s⁻¹.

BASE OH reactivity for Europe (Fig. 2) is lower, overall, than that of the United States, with only a few scattered maxima primarily associated with anthropogenic emissions near high population areas. We also note elevated BASE OH reactivity over Russia in 2010 as a result of widespread wildfires over the region that summer. This region in particular shows low or even negative changes in total OH reactivity due to drops in the extremely high levels of NO_x with additional VOC chemistry. Increases in reactivity from aromatics and monoterpenes are more homogeneous in Western Europe than in the United States, with increases between 0.2 s⁻¹ and 0.5 s⁻¹ throughout most of the region, representing relative increases of 4–20%.

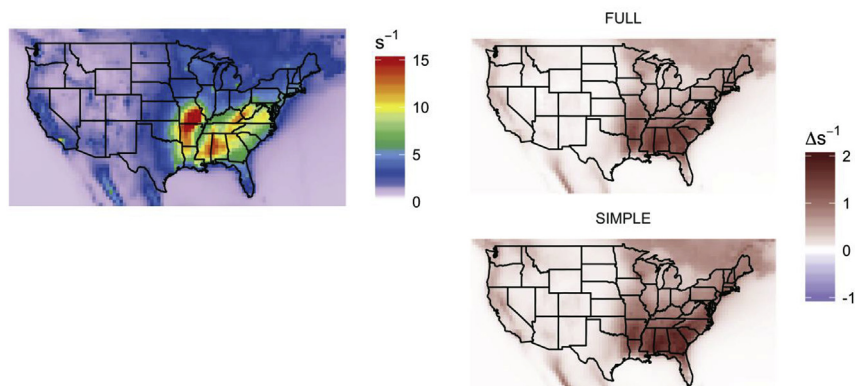
BASE case OH reactivity in China and Southeast Asia (Fig. 3) is heavily concentrated in the south and east, roughly following population density, with biogenic peaks to the south in Myanmar and Vietnam. Reactivity increases in China due to the addition of monoterpene and aromatic chemistry are most pronounced in the southeast, where changes average 0.4 s⁻¹, or 7% of BASE values. Negative changes in reactivity along the east coast from Beijing to Shanghai in the FULL case are again the result of decreases in the exceptionally high NO_x concentrations due to the additional chemical sinks provided by this mechanism.

Overall, increases in OH reactivity are similar between the FULL and SIMPLE cases, though magnitudes of changes are slightly higher in the SIMPLE cases (0.1 s⁻¹ higher on average across all

Table 1

Species added to FULL and SIMPLE GEOS-Chem simulations, with sources indicated by color.

FULL		SIMPLE	
Name	Description	Name	Description
BENZ	Benzene	BENZ	Benzene
TOLU	Toluene	TOLU	Toluene
XYLE	Xylene	XYLE	Xylene
BENP	Benzene peroxy radical	BENP	Benzene peroxy radical
TOLP	Toluene peroxy radical	TOLP	Toluene peroxy radical
XYLP	Xylene peroxy radical	XYLP	Xylene peroxy radical
CSL	Cresol	CSL	Cresol
PHEN	Phenol	PHEN	Phenol
BEPOMUC	Unsaturated epoxide-dialdehyde	EPX	Epoxide from BENZ
PHENO2	Bicyclic peroxy radical from OH addition to phenol	DCB	Unsaturated dicarbonyl
PHENO	Bicyclic oxy radical from OH addition to phenol	TCO3	Unsaturated acyl peroxy radical
PHENOOH	Bicyclic hydroperoxide from OH addition to phenol	MONX	Total monoterpenes
C6H5O2	C6H5O2	TERPO2	Terpene peroxy radicals
C6H5OOH	C6H5OOH	TERPOOH	Terpene hydroperoxide
BENZO2H	Bicyclic hydroperoxide from OH addition to benzene		
BIGALD1	Unsaturated dialdehyde		from Knote et al., 2014 (also in AROM case)
BIGALD2	Unsaturated dicarbonyl		from Fischer et al., 2016 (also in TERP case)
BIGALD3	Unsaturated dialdehyde		from (Goliff et al., 2013)
BIGALD4	Unsaturated dicarbonyls from xylene oxidation		from (Stockwell et al., 1990)
MALO2	Acyl radical from “BIGALD1” photolysis		from (Emmons et al., 2010)
PBZNIT	Peroxybenzoyl nitrate		
TEPOMUC	Unsaturated epoxide-dialdehyde		
BZOO	Peroxy radical formed following OH abstraction from toluene		
BZOOH	C6H5CH2OOH		
BZALD	Benzaldehyde		
ACBZO2	Acylperoxy radical obtained from benzaldehyde		
DICARBO2	Acylperoxy radical obtained from photolysis of unsaturated dicarbonyls		
MDIALO2	Acylperoxy radical obtained from photolysis of unsaturated dicarbonyls		
XYLOL	Isomers of C6H3(CH3)2(OH)		
XYLOLOOH	Bicyclic hydroperoxide from OH addition to xylenols		
XYLENO2	Bicyclic peroxy radicals from OH addition to xylenes		
XYLENOOH	Bicyclic hydroperoxides from OH addition to xylenes		
API	α -pinene, β -pinene, sabinene, and Δ -3-carene		
APIO2	Peroxy radical formed from API		
LIM	Limonene, myrcene, and ocimene		
LIMO2	Peroxy radical formed from LIM		
PIP	Peroxides from API & LIM		
OLND	monoterpene-derived NO ₃ -alkene adduct that primarily decomposes		
OLNN	monoterpene-derived NO ₃ -alkene adduct that primarily retains the NO ₃ functional group		
MONITS	saturated first-generation monoterpene organic nitrate		
MONITU	unsaturated first-generation monoterpene organic nitrate		
HONIT	second generation monoterpene organic nitrate		

**Fig. 1.** Average summer (JJA) surface OH reactivity for United States BASE case (left, saturated at 15 s^{-1}) and change to summed OH reactivity (right, saturated at 2 s^{-1}) for online aromatic and monoterpene chemistry using FULL and SIMPLE cases.

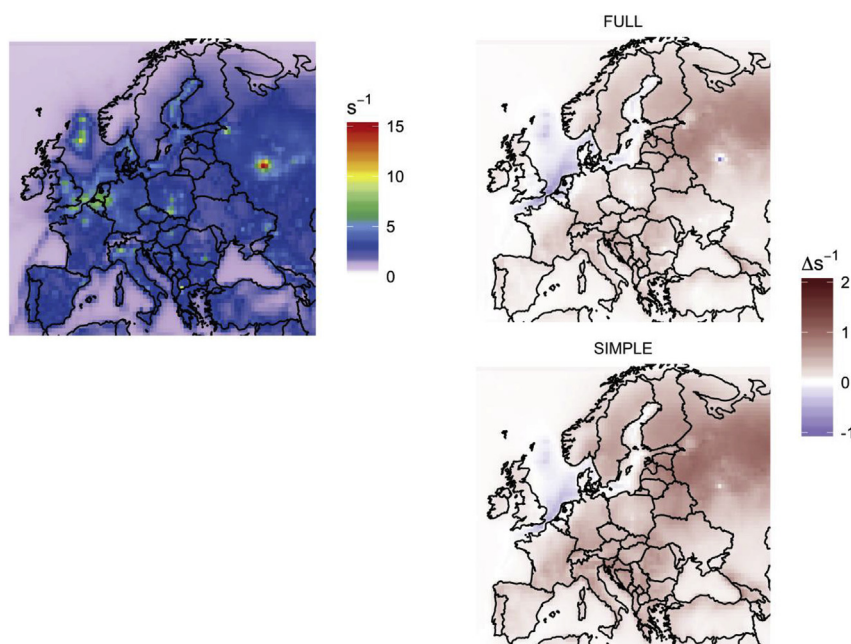


Fig. 2. As Fig. 1, for Europe region.

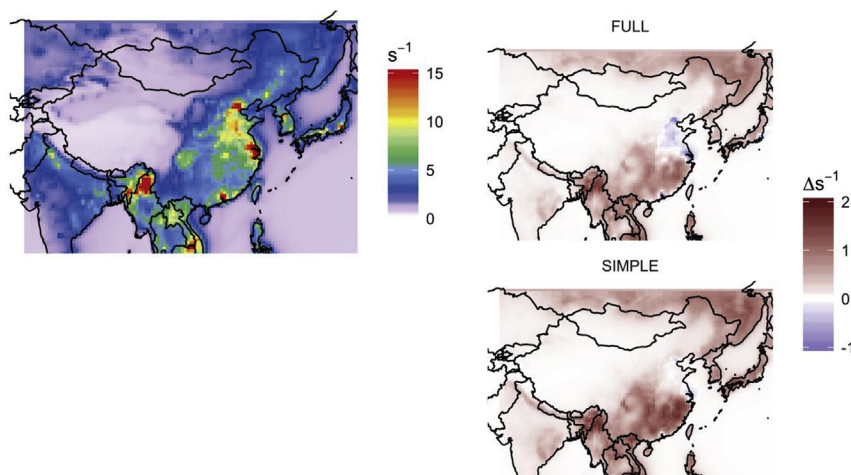


Fig. 3. As Fig. 1, for Asia region.

regions). This increased magnitude in the SIMPLE case is driven by two primary differences: differences in monoterpene oxidation products, and differences in NO_x sink efficiency. While the FULL case includes explicit bins for monoterpene oxidation products, the simplified SIMPLE case employs methyl vinyl ketone (MVK) and methacrolein (MACR). Differences in the reactivity and fate of the species in these two pathways end up leading to a net reactivity increase for the SIMPLE case in most regions. Furthermore, reaction pathways present in the FULL case tend to lead to greater removal of NO_x , for example via reaction with the phenol oxidation product PHENO, which does not exist in the SIMPLE case. In areas with extremely high NO_x levels, particularly in the Europe and Asia regions, this decrease in NO_x appears as a net decrease in total OH reactivity. While the FULL case adds reactive species and sinks that the SIMPLE case does not (Fig. 4), in most locations this is balanced by increases in other species. For example, while the FULL simulation contains two monoterpene species (API and LIM) and the

SIMPLE case uses only one (MONX) representing the binned sum of both FULL case species, total reactivity differences from the addition of these groups remains relatively balanced overall. On average, changes in these monoterpenes proved most relevant to changes in summed OH reactivity, as aromatic emissions are in general more localized. The additional aromatic and monoterpene species in both the FULL and SIMPLE cases, along with their products, contribute an additional 7–12% to the total summed surface OHR in each of the three regions, or 18–35% of the OH reactivity from VOCs.

The increases in total OH reactivity bring model results closer to observed totals, though large gaps do remain. In general, modeled summed OH reactivity is much lower than observations, mirroring the gap between observed and calculated reactivity in campaigns worldwide. For example, observed OH reactivities at forested sites in northern Michigan and Finland both showed mean measured OH reactivities of around $11\text{--}12\text{ s}^{-1}$, while the calculated reactivities

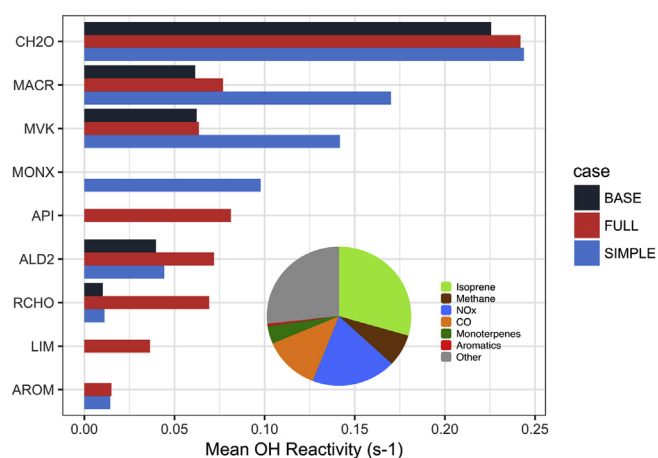


Fig. 4. Mean contribution of select species to total average surface summertime OH reactivity. Pie chart shows relative contributions to global terrestrial OH reactivity for FULL case, while bars highlight the OH reactivity of key species impacted by the addition of monoterpene and aromatic chemistry.

from the summation of known species contributions could explain only 30–50% of this, depending on the time of day (Hansen et al., 2014; Nölscher et al., 2012). Summed simulated summer reactivities for the grid cells containing these locations in the BASE case are each around 2.5 s⁻¹, and additional reactivity provided by the FULL case adds only 0.5 s⁻¹ to that value. Comparison to summer observations at urban sites in Houston and London show similar model underpredictions and relative changes (Mao et al., 2010; Whalley et al., 2016). Together, these results suggest that the inclusion of known aromatic and monoterpene chemistry is insufficient to significantly close the gap between observed and modeled OH reactivities.

While the additional OH reactivity provided by including aromatics and monoterpenes in the model does not close the gap between modeled and observed OH reactivities, it represents one step towards a better representation of observed behaviors. Additional improvements may be found through higher resolution simulations, as well as ongoing improvements to emission inventories and multi-generational oxidative chemistry. Previous studies have indicated that highly reactive hydrocarbons and secondary oxidation products missing from current inventories and mechanisms may be responsible for the large gaps in both calculated and modeled reactivity totals (Yang et al., 2016).

3.2. Increases in tropospheric O₃

In most locations, the increased OH reactivity produced by the inclusion of aromatics and monoterpenes leads to increases in surface O₃ levels as well, especially in regions rich in NO_x. These changes are significant; for example they are comparable to or larger than the impact of climate change on surface ozone concentrations (Tai et al., 2013). In the United States (Fig. 5), increases in daily maximum 8-h average summertime O₃ exceed 10 ppb over southern California with the addition of aromatics alone. For context, a change of 14 ppb O₃ (the maximum simulated increase due to the additional VOCs) is equivalent to 19% of the current 70 ppb EPA daily maximum 8-hr standard in the United States. Outside of southern California, increases of 0.5 ppb are apparent throughout most of the country in the FULL case (1.5 ppb in SIMPLE case), with the exception of the southeast, where VOC-insensitive O₃ production is consistent with high pre-existing VOC concentrations. Peak O₃ increases are largely driven by the additional

aromatic chemistry, though mean changes are strongly influenced by the additional monoterpene reactivity, due to greater area of impact. In Europe (Fig. 6), changes in O₃ are more uniform, showing few spatial features, and peaks at 5 ppb. In Asia, increases of around 4 ppb occur over eastern China and neighboring regions, where high existing NO_x concentrations enhance the impact of additional aromatic reactivity on O₃ levels (Fig. 7). Relatively small O₃ changes are observed in Burma and Thailand, where large increases in OH reactivity from monoterpenes do little to change an already VOC-saturated regime.

In all cases, changes in O₃ are heavily dependent on ambient NO_x/VOC ratios, as indicated by lower-left panels of Figs. 5–7. Here, the distribution of changes in O₃ are shown, divided into two categories based on the ratio of hydrogen peroxide (H₂O₂) vs. nitric acid (HNO₃). This ratio is a simple metric for estimating NO_x/VOC sensitivity, assuming that nitric acid is the main NO_x sink (Milford et al., 1994; Sillman et al., 1997). In each region, terrestrial grid cells in the bottom 50% of this ratio (indicating more VOC sensitivity) showed much more pronounced positive increases in O₃, while more VOC-saturated regions showed reduced O₃ increases, or even reductions associated with the addition of monoterpene and aromatic chemistry. This highlights how the response of ozone to additional VOC sources is strongly dependent on chemical environment. The SIMPLE implementation also shows stronger positive changes in O₃ in all three regions, averaging around 1 ppb higher values than found in the FULL case.

Comparison to O₃ observations through the EPA's AQS network of stations in the United States show mixed results. The BASE case simulation overpredicts O₃ at most sites (total mean bias of 8.2 ± 6.5 ppb). California's San Joaquin Valley region stands as one notable exception, where modeled O₃ actually underpredicts average summer observations for these years by up to 18 ppb. As would be expected, the additional O₃ generated by aromatic and monoterpene chemistry in most areas increases an already positive bias; the FULL case shows a total mean bias of 9 ppb, ±7 ppb. Exceptions to this can be found in California, where the previously noted O₃ underprediction is improved by an average of 1.6 ppb in the FULL case, as well as in the Southeast, where reductions in O₃ resulting from additional VOC reactivity in an already saturated region slightly improve agreement with observations. In Europe, BASE case comparison with observations from the EEA's AirBase inventory shows a similar overprediction of surface summertime O₃ of 9.5 ± 6.9 ppb. The additional VOC chemistry of the FULL case enhances this bias by an average of 2.0 ± 0.8 ppb.

Comparison of aromatic levels themselves to AQS observations (not shown) shows a modest overprediction in urban areas and a comparable underprediction in rural areas (overall bias of -0.03 ppb, RMSE of 0.45 ppb), differences which may stem from uncertainties in aromatic emissions inventories. Unfortunately, no such record of systematic observations exist for monoterpenes at this time, making a direct comparison of these modeled species impossible.

4. Conclusions

By integrating aromatics and monoterpenes into the GEOS-Chem gas-phase chemistry mechanism, we quantify the potential impacts of these species on total OH reactivity and O₃ production, finding important contributions to each. Although an already positive O₃ bias is exacerbated by the additional effective VOC burden, we find slightly improved agreement with observed OH reactivity totals, a metric that in general has shown a significant negative bias in model results. Furthermore, many uncertainties surround each step of O₃ formation, including precursor emissions, oxidative chemistry, transport, and removal. While the additional

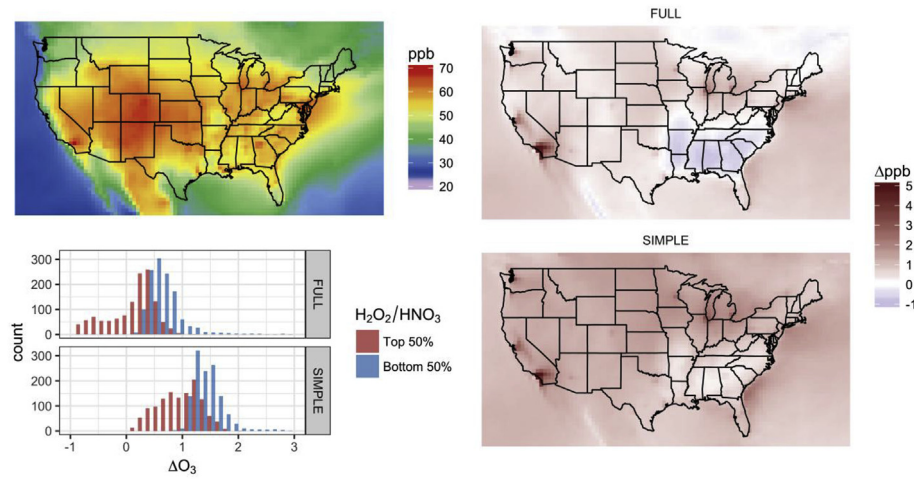


Fig. 5. Mean peak 8-h average O_3 in the United States summer (upper left), changes with additional VOC chemistry in FULL and SIMPLE cases (right), and the distribution of terrestrial O_3 changes for the FULL case (compared to BASE) segregated by mean simulated H_2O_2/HNO_3 ratio as a proxy representation of NO_x/VOC sensitivity (lower left). Histogram x-axis is trimmed for visibility. Full range of values extends from -1 ppb to 14 ppb (FULL) and 0 – 11 ppb (SIMPLE).

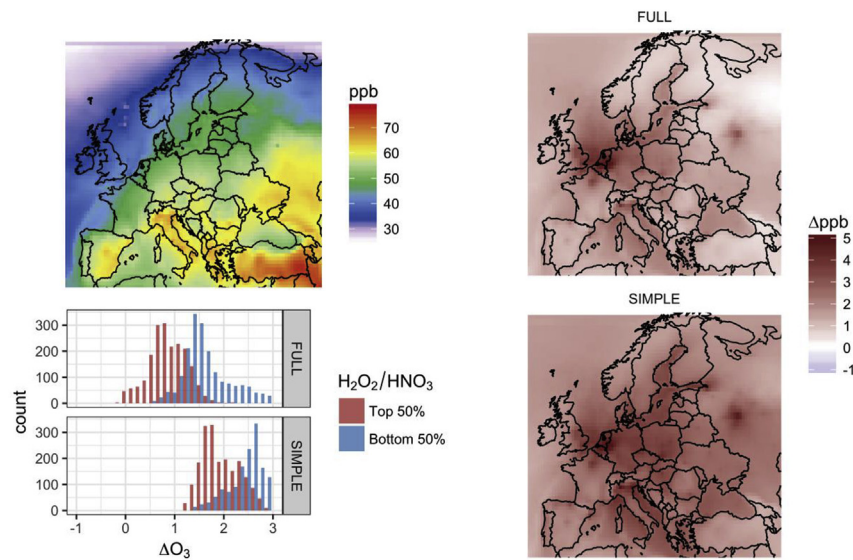


Fig. 6. As Fig. 5, for Europe. Histogram x-axis is trimmed for visibility. Full range of values extends from 0 ppb to 5 ppb (FULL) and 1 ppb– 4 ppb (SIMPLE).

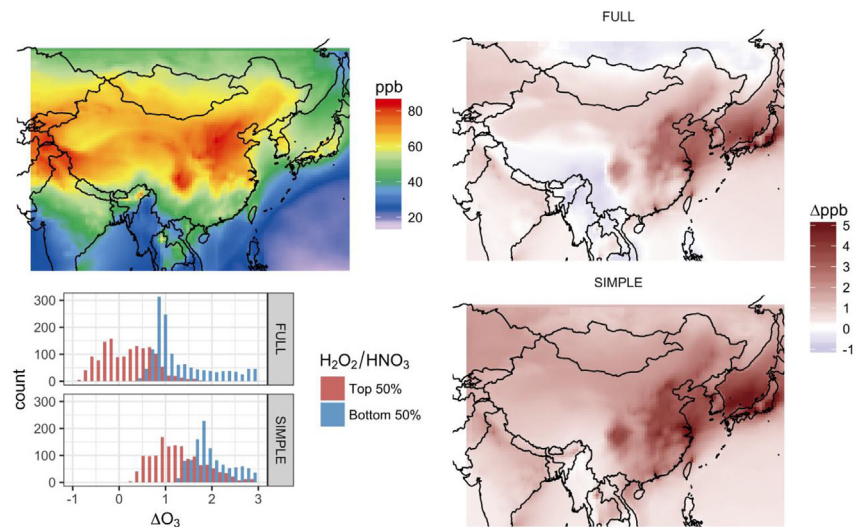


Fig. 7. As Fig. 5, for Asia. Histogram x-axis is trimmed for visibility. Full range of values extends from -1 ppb to 4 ppb (FULL) and 0 ppb– 6 ppb (SIMPLE).

reactivity provided by bringing these species online pushes over-predicted O₃ even higher in these simulations, other ongoing and proposed changes such as the addition of halogen chemistry (Sherwen et al., 2016), may reduce O₃ values, making the additional production from aromatics and monoterpenes more beneficial to model skill. For these reasons, we propose that the inclusion of aromatic and monoterpene chemistry is important for the effective representation and prediction of ozone pollution, despite substantial uncertainties regarding product distribution and rates of multigenerational chemistry. While the inclusion of additional advected species increases computational demands, we show that this can be mitigated through a simplified representation of this chemistry, representing the increased OH reactivity with less computational cost. To further optimize these improvements, future laboratory experiments targeting the relevant chemical kinetics will be necessary, along with ongoing efforts to develop a robust, efficient, and accurate chemical mechanism for the representation of these products and their reactions in large-scale models.

Acknowledgements

This work was supported by NSF (ATM-1564495) and NOAA (NA14OAR4310132).

Appendix A. Supplementary data

Supplementary data related to this article can be found at <https://doi.org/10.1016/j.atmosenv.2017.08.048>.

References

- Auvray, M., Bey, I., 2005. Long-range transport to Europe: seasonal variations and implications for the European ozone budget. *J. Geophys. Res. Atmos.* 110, D11303. <http://dx.doi.org/10.1029/2004JD005503>.
- Cooper, O.R., Parrish, D.D., Ziemke, J., Balashov, N.V., Cupeiro, M., Galbally, I.E., Gilge, S., Horowitz, L., Jensen, N.R., Lamarque, J.-F., Naik, V., Oltmans, S.J., Schwab, J., Shindell, D.T., Thompson, A.M., Thouret, V., Wang, Y., Zbinden, R.M., 2014. Global distribution and trends of tropospheric ozone: an observation-based review. *Elementa* 2. <http://dx.doi.org/10.12952/journal.elementa.000029>.
- Fisher, J.A., Jacob, D.J., Travis, K.R., Kim, P.S., Marais, E.A., Chan Miller, C., Yu, K., Zhu, L., Yantosca, R.M., Sulprizio, M.P., Mao, J., Wennberg, P.O., Crounse, J.D., Teng, A.P., Nguyen, T.B., St. Clair, J.M., Cohen, R.C., Romer, P., Nault, B.A., Wooldridge, P.J., Jimenez, J.L., Campuzano-Jost, P., Day, D.A., Hu, W., Shepson, P.B., Xiong, F., Blake, D.R., Goldstein, A.H., Misztal, P.K., Hanisco, T.F., Wolfe, G.M., Ryerson, T.B., Wisthaler, A., Mikoviny, T., 2016. Organic nitrate chemistry and its implications for nitrogen budgets in an isoprene- and monoterpene-rich atmosphere: constraints from aircraft (SEAC4RS) and ground-based (SOAS) observations in the Southeast US. *Atmos. Chem. Phys.* 16, 5969–5991. <http://dx.doi.org/10.5194/acp-16-5969-2016>.
- Goldstein, A.H., Galbally, I.E., 2007. Known and unexplored organic constituents in the Earth's atmosphere. *Env. Sci. Technol.* 41, 1514–1521. <http://dx.doi.org/10.1021/es072476p>.
- Guenther, A., Karl, T., Harley, P., Wiedinmyer, C., Palmer, P.I., Geron, C., 2006. Estimates of global terrestrial isoprene emissions using MEGAN (model of emissions of gases and aerosols from nature). *Atmos. Chem. Phys. Discuss.* 6, 107–173. <http://dx.doi.org/10.5194/acpd-6-107-2006>.
- Guenther, A.B., Jiang, X., Heald, C.L., Sakulyanontvittaya, T., Duhl, T., Emmons, L.K., Wang, X., 2012. The Model of Emissions of Gases and Aerosols from Nature version 2.1 (MEGAN2.1): an extended and updated framework for modeling biogenic emissions. *Geosci. Model Dev.* 5, 1471–1492. <http://dx.doi.org/10.5194/gmd-5-1471-2012>.
- Guerreiro, C.B.B., Foltescu, V., de Leeuw, F., 2014. Air quality status and trends in Europe. *Atmos. Environ.* 98, 376–384. <http://dx.doi.org/10.1016/j.atmosenv.2014.09.017>.
- Hansen, R.F., Griffith, S.M., Dusanter, S., Rickly, P.S., Stevens, P.S., Bertman, S.B., Carroll, M.A., Erickson, M.H., Flynn, J.H., Grossberg, N., Jobson, B.T., Lefer, B.L., Wallace, H.W., 2014. Measurements of total hydroxyl radical reactivity during CABINEX 2009 – Part 1: field measurements. *Atmos. Chem. Phys.* 14, 2923–2937. <http://dx.doi.org/10.5194/acp-14-2923-2014>.
- Jenkin, M.E., Clemitshaw, K.C., 2000. Ozone and other secondary photochemical pollutants: chemical processes governing their formation in the planetary boundary layer. *Atmos. Environ.* 34, 2499–2527. [http://dx.doi.org/10.1016/S1352-2310\(99\)00478-1](http://dx.doi.org/10.1016/S1352-2310(99)00478-1).
- Knote, C., Hodzic, A., Jimenez, J.L., Volkamer, R., Orlando, J.J., Baidar, S., Brioude, J., Fast, J., Gentner, D.R., Goldstein, A.H., Hayes, P.L., Knighton, W.B., Oetjen, H., Setyan, A., Stark, H., Thalman, R., Tyndall, G., Washenfelder, R., Waxman, E., Zhang, Q., 2014. Simulation of semi-explicit mechanisms of SOA formation from glyoxal in aerosol in a 3-D model. *Atmos. Chem. Phys.* 14, 6213–6239. <http://dx.doi.org/10.5194/acp-14-6213-2014>.
- Kuhns, H., Knipping, E.M., Vukovich, J.M., 2005. Development of a United States–Mexico emissions inventory for the big bend regional aerosol and visibility observational (BRAVO) study. *J. Air Waste Manag. Assoc.* 55, 677–692. <http://dx.doi.org/10.1080/10473289.2005.10464648>.
- Lim, S.S., et al., 2012. A comparative risk assessment of burden of disease and injury attributable to 67 risk factors and risk factor clusters in 21 regions, 1990–2010: a systematic analysis for the Global Burden of Disease Study 2010. *Lancet* 380, 2224–2260. [http://dx.doi.org/10.1016/S0140-6736\(12\)61766-8](http://dx.doi.org/10.1016/S0140-6736(12)61766-8).
- Mao, J., Ren, X., Chen, S., Brune, W.H., Chen, Z., Martinez, M., Harder, H., Lefer, B., Rappenglück, B., Flynn, J., Leuchner, M., 2010. Atmospheric oxidation capacity in the summer of Houston 2006: comparison with summer measurements in other metropolitan studies. *Atmos. Environ.* 44, 4107–4115. <http://dx.doi.org/10.1016/j.atmosenv.2009.01.013>.
- Milford, J.B., Gao, D., Sillman, S., Blossy, P., Russell, A.G., 1994. Total reactive nitrogen (NO_y) as an indicator of the sensitivity of ozone to reductions in hydrocarbon and NO_x emissions. *J. Geophys. Res. Atmos.* 99, 3533–3542. <http://dx.doi.org/10.1029/93JD03224>.
- Mu, M., Randerson, J.T., van der Werf, G.R., Giglio, L., Kasibhatla, P., Morton, D., Collatz, G.J., DeFries, R.S., Hyer, E.J., Prins, E.M., Griffith, D.W.T., Wunch, D., Toon, G.C., Sherlock, V., Wennberg, P.O., 2011. Daily and Hourly Variability in Global Fire Emissions and Consequences for Atmospheric Model Predictions of Carbon Monoxide.
- Nölscher, A.C., Williams, J., Sinha, V., Custer, T., Song, W., Johnson, A.M., Axinte, R., Bozem, H., Fischer, H., Pouvesle, N., Phillips, G., Crowley, J.N., Rantala, P., Rinne, J., Kulmala, M., Gonzales, D., Valverde-Canossa, J., Vogel, A., Hoffmann, T., Ouwersloot, H.G., Vilà-Guerau de Arellano, J., Lelieveld, J., 2012. Summertime total OH reactivity measurements from boreal forest during HUMPPA-COPEC 2010. *Atmos. Chem. Phys.* 12, 8257–8270. <http://dx.doi.org/10.5194/acp-12-8257-2012>.
- Olivier, J.G.J., Berdowski, J.J.M., 2001. Global emission sources and sinks. In: *The Climate System. A. A. Balkema Publishers/Swets & Zeitlinger, Lisse, The Netherlands*, pp. 33–78.
- Paulot, F., Crounse, J.D., Kjaergaard, H.G., Kroll, J.H., Seinfeld, J.H., Wennberg, P.O., 2009a. Isoprene photooxidation: new insights into the production of acids and organic nitrates. *Atmos. Chem. Phys.* 9, 1479–1501. <http://dx.doi.org/10.5194/acp-9-1479-2009>.
- Paulot, F., Crounse, J.D., Kjaergaard, H.G., Kürten, A., St. Clair, J.M., Seinfeld, J.H., Wennberg, P.O., 2009b. Unexpected epoxide formation in the gas-phase photooxidation of isoprene. *Science* 325, 730–733. <http://dx.doi.org/10.1126/science.1172910>.
- Piccot, S.D., Watson, J.J., Jones, J.W., 1992. A global inventory of volatile organic compound emissions from anthropogenic sources. *J. Geophys. Res. Atmos.* 97, 9897–9912. <http://dx.doi.org/10.1029/92JD00682>.
- Pulles, T., van het Bolscher, M., Brand, R., Visschedijk, A., 2007. Assessment of Global Emissions from Fuel Combustion in the Final Decades of the 20th Century.
- Pye, H.O.T., Chan, A.W.H., Barkley, M.P., Seinfeld, J.H., 2010. Global modeling of organic aerosol: the importance of reactive nitrogen (NO_x and NO_y). *Atmos. Chem. Phys.* 10, 11261–11276. <http://dx.doi.org/10.5194/acp-10-11261-2010>.
- Safieddine, S.A., Heald, C.L., Henderson, B.H., 2017. The global nonmethane reactive organic carbon budget: a modeling perspective. *Geophys. Res. Lett.* <http://dx.doi.org/10.1002/2017GL072602>, 2017GL072602.
- Sherwen, T., Schmidt, J.A., Evans, M.J., Carpenter, L.J., Großmann, K., Eastham, S.D., Jacob, D.J., Dix, B., Koenig, T.K., Sinreich, R., Ortega, I., Volkamer, R., Saiz-Lopez, A., Prados-Roman, C., Mahajan, A.S., Ordóñez, C., 2016. Global impacts of tropospheric halogens (Cl, Br, I) on oxidants and composition in GEOS-Chem. *Atmos. Chem. Phys.* 16, 12239–12271. <http://dx.doi.org/10.5194/acp-16-12239-2016>.
- Sillman, S., He, D., Cardelino, C., Imhoff, R.E., 1997. The use of photochemical indicators to evaluate ozone-NO_x-hydrocarbon sensitivity: case studies from Atlanta, New York, and Los Angeles. *J. Air Waste Manag. Assoc.* 47, 1030–1040. <http://dx.doi.org/10.1080/10473289.1997.10464407>.
- Simon, H., Reff, A., Wells, B., Xing, J., Frank, N., 2015. Ozone trends across the United States over a period of decreasing NO_x and VOC emissions. *Environ. Sci. Technol.* 49, 186–195. <http://dx.doi.org/10.1021/es504514z>.
- Tai, A.P.K., Mickley, L.J., Heald, C.L., Wu, S., 2013. Effect of CO₂ inhibition on biogenic isoprene emission: implications for air quality under 2000 to 2050 changes in climate, vegetation, and land use: CO₂-isoprene interaction and air quality. *Geophys. Res. Lett.* 40, 3479–3483. <http://dx.doi.org/10.1002/grl.50650>.
- Travis, K.R., Jacob, D.J., Fisher, J.A., Kim, P.S., Marais, E.A., Zhu, L., Yu, K., Miller, C.C., Yantosca, R.M., Sulprizio, M.P., Thompson, A.M., Wennberg, P.O., Crounse, J.D., St. Clair, J.M., Cohen, R.C., Laughner, J.L., Dibb, J.E., Hall, S.R., Ullmann, K., Wolfe, G.M., Pollack, I.B., Peischl, J., Neuman, J.A., Zhou, X., 2016. Why do models overestimate surface ozone in the Southeast United States? *Atmos. Chem. Phys.* 16, 13561–13577. <http://dx.doi.org/10.5194/acp-16-13561-2016>.
- US Environmental Protection Agency, n.d. Air Quality System Data Mart [internet database] [WWW Document]. AQS Data Mart. URL https://aqs.epa.gov/aqsweb/documents/data_mart_welcome.html (accessed 8.9.16).
- Whalley, L.K., Stone, D., Bandy, B., Dunmore, R., Hamilton, J.F., Hopkins, J., Lee, J.D., Lewis, A.C., Heard, D.E., 2016. Atmospheric OH reactivity in central London: observations, model predictions and estimates of in situ ozone production.

- Atmos. Chem. Phys. 16, 2109–2122. <http://dx.doi.org/10.5194/acp-16-2109-2016>.
- Xiao, Y., Logan, J.A., Jacob, D.J., Hudman, R.C., Yantosca, R., Blake, D.R., 2008. Global budget of ethane and regional constraints on U.S. sources. *J. Geophys. Res. Atmos.* 113, D21306. <http://dx.doi.org/10.1029/2007JD009415>.
- Yang, Y., Shao, M., Wang, X., Nölscher, A.C., Kessel, S., Guenther, A., Williams, J., 2016. Towards a quantitative understanding of total OH reactivity: a review. *Atmos. Environ.* 134, 147–161. <http://dx.doi.org/10.1016/j.atmosenv.2016.03.010>.
- Zhang, Q., Streets, D.G., Carmichael, G.R., He, K.B., Huo, H., Kannari, A., Klimont, Z., Park, I.S., Reddy, S., Fu, J.S., Chen, D., Duan, L., Lei, Y., Wang, L.T., Yao, Z.L., 2009. Asian emissions in 2006 for the NASA INTEX-B mission. *Atmos. Chem. Phys.* 9, 5131–5153. <http://dx.doi.org/10.5194/acp-9-5131-2009>.

Further reading

- Emmons, L.K., Walters, S., Hess, P.G., Lamarque, J.-F., Pfister, G.G., Fillmore, D., Granier, C., Guenther, A., Kinnison, D., Laepple, T., Orlando, J., Tie, X., Tyndall, G., Wiedinmyer, C., Baughcum, S.L., Kloster, S., 2010. Description and evaluation of the model for ozone and related chemical tracers, version 4 (MOZART-4). *Geosci. Model Dev.* 3, 43–67. <http://dx.doi.org/10.5194/gmd-3-43-2010>.
- Goliff, W.S., Stockwell, W.R., Lawson, C.V., 2013. The regional atmospheric chemistry mechanism, version 2. *Atmos. Environ.* 68, 174–185. <http://dx.doi.org/10.1016/j.atmosenv.2012.11.038>.
- Stockwell, W.R., Middleton, P., Chang, J.S., Tang, X., 1990. The second generation regional acid deposition model chemical mechanism for regional air quality modeling. *J. Geophys. Res. Atmos.* 95, 16343–16367. <http://dx.doi.org/10.1029/JD095iD10p16343>.